10 Tb/s PM-64QAM Self-Homodyne Comb-Based Superchannel Transmission With 4% Shared Pilot Tone Overhead

Mikael Mazur, *Student Member, OSA*, Abel Lorences-Riesgo, Jochen Schröder, *Member, IEEE, Member, OSA*, Peter A. Andrekson, *Fellow, IEEE, Fellow, OSA*, and Magnus Karlsson, *Senior Member, IEEE, Fellow, OSA*

***Abstract*—We demonstrate transmission of a comb-based 10 Tb/s 50 × 20 Gbaud PM-64QAM superchannel using frequency comb regeneration to reduce carrier offsets and allow for self-homodyne detection. The regeneration is enabled by transmitting two optical pilot tones which are filtered and recovered in the receiver using optical injection locking and an electrical phase-locked loop. We show that by utilizing frequency combs together with optical pilot tones, self-homodyne detection similar to systems using one pilot tone per wavelength channel, can be achieved. Sharing the overhead for pilot tones reduces the complexity and limits the overhead to 4%. This enabled a total superchannel spectral efficiency of 7.7 b/s/Hz. To evaluate the performance, we perform both back-to-back measurements and transmission over 80 km of standard single-mode fiber. Successful self-homodyne detection of all 50 data channels in the 10-nm-wide superchannel demonstrates that the spectral coherence from frequency combs, combined with the use of optical pilots, can overcome limitations arising from frequency offset and phase noise in high-order QAM transmission while keeping the pilot overhead low.**

***Index Terms*—Analog optical signal processing, coherent communications, homodyning.**

I. Introduction

FUTURE demands in optical backbone network throughput requires cost-efficient solutions to increase the information rate per carrier. High spectral-efficiency transmission using higher-order polarization-multiplexed M-ary quadrature amplitude modulation (PM-MQAM) formats enables an increase in network throughput without deploying additional fibers. With this increase in modulation order follows increased sensitivity to both transceiver impairments and channel distortions and to mitigate these effects and ensure reliable communication, high performance digital signal processing (DSP) is needed [1].

Wavelength-division multiplexing (WDM) transmission is a key enabler of high-throughput transmission systems by enabling transmission of multiple parallel channels. The use of many wavelength channels allows for efficient use of the broad transmission spectrum provided by optical fibers together with erbium-doped fiber amplifiers (EDFAs), which spans several THz and is orders of magnitude larger than the electrical bandwidth of, for example, state-of-the-art modulators [2]. As both the number of channels and the modulation order grow, so does the cost for high quality lasers required to enable DSP-based carrier recovery without risking critical cyclic-slip events. Even though the price for external cavity lasers with linewidth of around 10–100 kHz is getting lower and the energy consumption for digital phase tracking is on the order of a few percent for long-haul systems [3], both cost and energy scale linearly with the number of channels. Furthermore, pilot-aided DSP-based phase tracking for modulation formats such as 64QAM uses around 4% pilot symbols for lasers with about 100 kHz linewidth to track the phase noise and avoid cycle slips [4]. In fully loaded systems, commonly employing more than 100 separate wavelength channels per spatial mode [5], significant savings in energy and/or increased system throughput can be achieved by utilizing schemes for sharing resources among several carriers to reduce the final cost per transmitted bit [6], [7].

Self-homodyne detection with a polarization-multiplexed pilot tone has previously been suggested to avoid DSP-based frequency offset and phase noise compensation at the expense of lost spectral efficiency (SE) due to the requirement of transmitting the pilot [8]. Polarization-multiplexing of the pilot tone implies a 50% loss in SE and to reduce this, schemes such as interleaved pilot transmission [9] and the use of multi-core fibers [10] have been proposed. In the case of multi-core fiber transmission, only one single laser is used per wavelength channel and then shared among all cores, apart from a single core dedicated for pilot tone transmission and the resulting overhead is inversely proportional to the number of cores available. Self-homodyne detection combined with multi-core fiber transmission has also been studied for systems using conventional blind digital phase tracking and has been shown to reduce the required estimation rate by up to 3 orders of magnitude [11]. For systems using digital pilot-symbol based phase tracking,

Manuscript received October 2, 2018; revised January 12, 2018; accepted March 23, 2018. Date of publication March 28, 2018; date of current version June 19, 2018. This work was supported by the Swedish Research Council under Grant 2014-06138. *(Corresponding author: Mikael Mazur.)*

M. Mazur, J. Schröder, P. A. Andrekson, and M. Karlsson are with the Photonics Laboratory, Fibre Optic Communication Research Centre, Department of Microtechnology and Nanoscience, Chalmers University of Technology, Gothenburg SE-412 96, Sweden (e-mail: mikael.mazur@chalmers.se; jochen.schroeder@chalmers.se; peter.andrekson@chalmers.se; magnus.karlsson@chalmers.se).

A. Lorences-Riesgo is with the Photonics Laboratory, Fibre Optic Communication Research Centre, Department of Microtechnology and Nanoscience, Chalmers University of Technology, Gothenburg SE-412 96, Sweden, and also with the IT-Instituto de Telecomunicações, 3810-193 Aveiro, Portugal (e-mail: abellorences@av.it.pt).

Color versions of one or more of the figures in this paper are available online at http://ieeexplore.ieee.org.

Digital Object Identifier 10.1109/JLT.2018.2820166

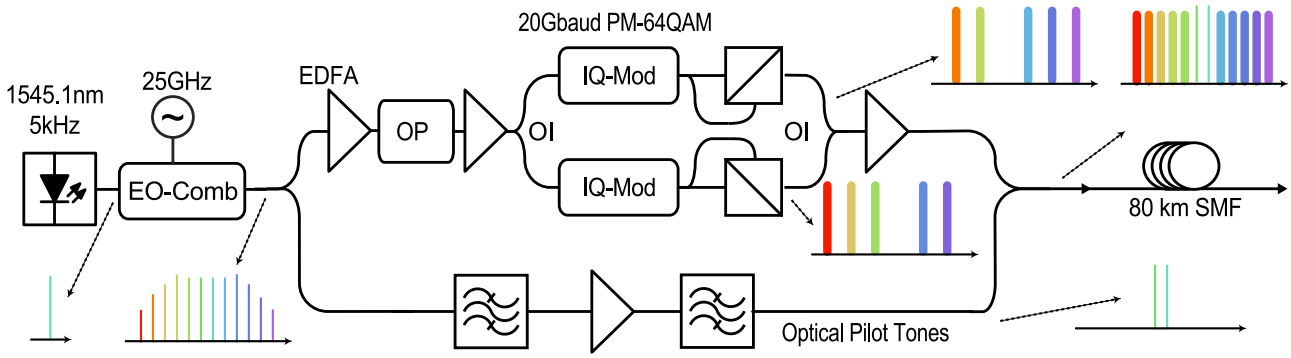

Fig. 1. Schematic picture of the 52 carrier, 10 Tb/s superchannel transmitter setup. All carriers originate from a single electro-optic frequency comb with 25 GHz spacing. Two carriers are separated and used as pilot tones to transmit the comb state to the receiver. The remaining 50 carriers are separated into even and odd carriers and modulated with 20 Gbaud PM-64QAM using two independent modulators. After modulation and polarization-multiplexing emulation, the data channels are combined with the pilot tones to form the final superchannel.

the effective suppression of laser phase noise translates into a relaxation in required pilot overhead (OH) [12]. In practice, the number of cores in a multi-core fiber is limited and inter-core skew fluctuations affect the effective path matching [13]. This causes reduction in the effective phase noise suppression for self-homodyne systems using the spatial domain for pilot-tone transmission [14]. Furthermore, the need to dedicate a complete core for pilot tone transmission will lead to OHs that are larger than the equivalent case of using individual digital pilot symbols for each wavelength channel unless a multi-core fiber with more than about 10 cores is used [4]. Moreover, this approach is incompatible with current systems using standard single-mode fiber (SSMF).

While implying a natural loss in spectral efficiency, the use of optical pilot tones can lead to a drastic reduction in linewidth requirements for system using sensitive modulation formats [11]. Transmission of a 2048QAM signal reaching a SE of 15.3 bits/s/Hz using a frequency-shifted pilot tone and an optical phase-locked loop has been demonstrated [15]. Here the use of an optical pilot tone replaced the usage of DSP-based frequency and phase tracking, which becomes increasingly complex as the modulation order gets larger [16], [17]. Despite this advantage, the baudrate was limited to 3 Gbaud due to the very high requirements of the digital to analog (DAC) and analogue to digital converter (ADC).

An alternative to reduce the number of high-quality laser sources for a WDM system with many channels is to use an optical frequency comb which provides multiple phase-locked carriers at a given spacing. This enables very dense packing of wavelength carriers and was exploited in [18] where the authors demonstrated a record throughput of 2.15 Pb/s using 399 WDM channels in a 22-core fiber. If a system employs frequency combs, its phase coherence can be exploited beyond the replacement of free-running lasers with frequency stable carriers. One such example is the use of phase-locked transmitter and receiver combs which enables homodyne detection of all channels [19]. Phase-locking of the transmitter and receiver combs requires information of the transmitter comb state to be transmitted to the receiver side. To fully characterize a frequency comb, both the optical phase from its central line and the frequency spacing is needed and hence has to be transmitted. One approach to phase-lock a receiver comb to a transmitter comb using a single unmodulated carrier and optical injection locking (OIL) was proposed in [20] where the authors only addressed the recovery and the central tone and not the frequency spacing set by the clock driving the frequency combs. To overcome this limitation, regeneration of the transmitter comb using two unmodulated tones, OIL and a parametric mixer was studied in [21] by means of linewidth scaling for the regenerated carriers. The first demonstration of data transmission using a homodyne superchannel was done in [19] where the concept from [21] was further expanded using Brillouin amplification to achieve narrow-band filtering of the pilot tones before parametric comb regeneration enabled self-homodyne detection of a 24 carrier PM-32QAM superchannel.

This work expands [22] where we have proposed the use of an electrical phase-locked loop (PLL) to achieve effective recovery of the pilot tones. We provide a detailed analysis of the PLL performance and its role in enabling self-homodyne detection of 50 $\times$ 20 Gbaud PM-64QAM superchannel. We also present a detailed back to back (B2B) characterization of the system performance and a more detailed study of the performance observed in the single-span transmission experiment. Locking of the transmitter and receiver combs is demonstrated using only 2 optical pilot tones, resulting in an overhead of 4% for self-homodyne detection which is directly comparable to the overhead of using digital pilot symbols in single-core fiber transmission.

II. Experimental Setup

An overview of the transmitter setup, the frequency comb spectra and the receiver structure including the comb regeneration setup can be seen in Fig. 1–4, respectively. In total we used 52 carriers, originating from a single frequency comb to form the superchannel. Out of these, 50 were used to transmit data and 2 were left without data modulation to enable regeneration of the phase-locked receiver comb. The superchannel spectral efficiency was 7.7 bits/s/Hz with a total net transmission rate of 10 Tbit/s assuming a 20% OH for forward error correction (FEC).

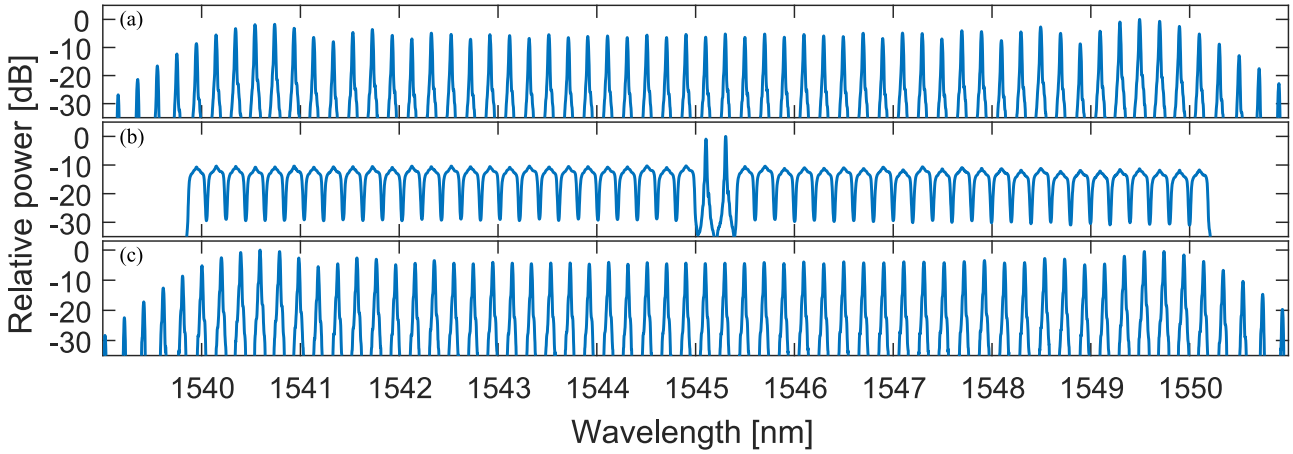

Fig. 2. Spectra of (a) transmitter frequency comb, (b) formed superchannel after combining 50 data carriers with the 2 pilot tones and (c) receiver frequency comb. All lines are modulated using 20 Gbaud PM-64QAM and the spectrums were measured using 0.01 nm resolution.

A. Transmitter

The transmitter is outlined in Fig. 1. We used a 5 kHz linewidth laser centered at 1545.12 nm to feed an electro-optic (EO) comb consisting of 2 phase modulators followed by an intensity modulator, similar to the EO-comb used in [23]. All modulators were driven by a single 25 GHz radio-frequency (RF) clock and the resulting spectrum can be seen in Fig. 2(a). The output of the comb was amplified and fed to an optical processor (OP) used to remove the two central carriers (1545.12 nm and 1545.32 nm), the out of band noise and to flatten the about 15 dB gain variations of the post OP amplifier. An optical interleaver (OI) was then used to separate the lines into even and odd lines. The even and odd lines were modulated using two separate IQ-modulators driven by 4 independent DACs operating at 60 Gs/s to modulate 20 Gbaud 64-QAM data shaped using a root-raised cosine filter with a roll-off factor of 5%. The pattern consisted of 2^{16} randomly chosen symbols. We digitally compensated for the DAC frequency response by applying its inverse response in the frequency domain and for the nonlinear transfer function of the modulator by applying the inverse response function. After polarization-multiplexing emulation using a split-combine step with approximately 100 symbols delay, odd and even channels were combined using a second OI before joint amplification and transmission.

To separate out the unmodulated carriers we used a 10 dB tap directly on the comb output followed by a 1 nm filter, an EDFA and a second 0.3 nm filter to isolate the two central carriers. The filter combination ensured a side-carrier suppression of >30 dB which was shown to be sufficient to not result in any significant penalty for the neighboring data channels, as shown in Section III-B. The unmodulated lines were then combined with the data carriers and the output spectrum of the combined signal is shown in Fig. 2(b). The power of the unmodulated carriers was tuned to have the same power per line as the data carriers. We note that the optimal power ratio will depend on several conditions such as link and recovery stage design; however, any detailed optimization of this was beyond the scope of this work equal launch power was therefore used. We evaluated the signal in B2B configuration and after transmission over one span of 80 km SSMF with about 16 dB of loss.

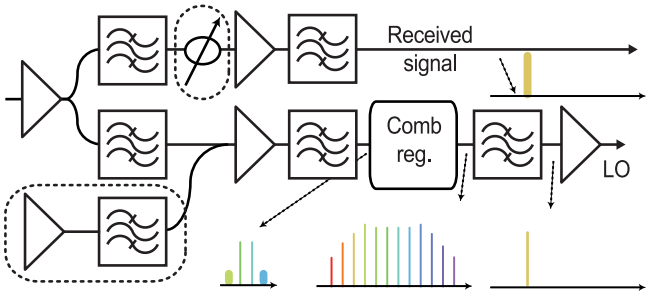

Fig. 3. Schematic of the receiver structure used to separate data channels from pilot tones. The pilot tones are then used for regenerating a phase-locked receiver comb from which an LO-line is extracted and used for self-homodyne detection of the selected data channel. Dashed components denotes components used in the noise-loading evaluation.

B. Receiver

The receiver structure is outlined in Fig. 3. After amplification we separated the received superchannel into two paths. One path is used to filter out the data channel and one to extract the two optical pilot tones. In the B2B configuration, noise loading was implemented independently for the data carriers and the pilot tones. The data carriers were noise loaded by inserting a variable optical attenuator (VOA) after the first filter in the upper arm of Fig. 3. Noise loading of the pilot tones was implemented by by combining them with additional noised generated by filtering the output noise of an EDFA using a 3 dB coupler after the first filter in the lower arm in Fig. 3.

To extract the data channel we used a tunable 0.2 nm filter followed by an EDFA and a 0.9 nm filter before detection. The two optical pilots were filtered out by cascading a 0.3 nm filter, an EDFA and a 0.9 nm filter. The filtered output was fed to the comb regeneration stage described in Section II-C, in which a frequency comb phase-locked to the transmitter comb was generated for usage as local oscillator (LO). To ensure sufficient LO power into the coherent receiver, the LO line corresponding

to the selected data channel was filtered using a 0.1 nm filter prior to amplification. The signal and LO were then combined in a standard coherent receiver.

The electrical outputs from the coherent receiver were sampled using a 50 GS/s real-time oscilloscope and DSP was implemented offline. The DSP consisted of initial front-end imbalance correction, low-pass filtering, re-sampling to 2 samples per symbol and equalization. The equalizer was divided between a static dispersion compensating equalizer (in the case of single-span transmission) and a dynamic decision-directed least mean square (DD-LMS) equalizer using 25 T/2-spaced taps. A constant modulus algorithm was used for pre-convergence over 10^5 symbols before switching to decision directed operation. Both equalizers used a step-size of $\mu = 4 \cdot 10^{-4}$ working on power-normalized constellations. Neither carrier frequency offset estimation nor phase recovery were needed and all residual phase fluctuations occurring from thermal drifts of fibers etc. were slow enough to be tracked by the dynamic equalizer.

To evaluate system performance we calculated both bit error ratio (BER) and generalized mutual information (GMI). We assumed a pre-FEC target of 5.7dB Q [24], or equivalently a BER of $2.7 \cdot 10^{-2}$[18], for binary soft-decision forward error correction with 20% OH. To further validate the performance we calculated the GMI, which has been shown to be a more accurate predictor for performance after SD-FEC decoding, assuming AWGN contributions [25]. The AWGN assumption is typically used both when designing the code and the corresponding de-mapper used to calculate the required L-values for SD decoding. As an important implication of this, the accuracy of GMI as well as the performance of any code designed for an AWGN channel can deviate for a non-AWGN channel. The GMI corresponds to the maximum possible throughput of a channel assuming the usage of optimal bit-wise SD-FEC together with a memory less receiver. Here we calculated the GMI by first estimating the received signal to noise ratio (SNR) of the received symbols (assuming $i.i.d.$ Gaussian noise contribution). Using the SNR we then calculated the L-values for soft de-mapping of the individual bits within the 64-QAM symbols ([25, eq. 29]). The bit-wise GMI was then estimated using the L-values together with the transmitted symbols ([25, eq. 30]) and the total GMI per 4D symbol by summing the individual GMI values over both polarizations. In this work we calculated the GMI from $2 \cdot 10^5$ symbols and BER using $1.2 \cdot 10^6$ demapped bits.

C. Comb Regeneration

The receiver comb was built the same way as the transmitter comb but had a lower maximum input power of 20 dBm. To regenerate a phase-locked receiver EO-comb, both the laser feeding the comb and the RF clock used to feed the modulators need to be phase-locked to the corresponding laser and clock feeding the transmitter comb. The comb recovery setup is shown in Fig. 4. After initial filtering and amplification (described in Section II-B) we used a 25 GHz OI to separate the two pilot tones into two arms. OIL was used to lock two slave lasers (standard distributed feedback lasers with free-running linewidth of about

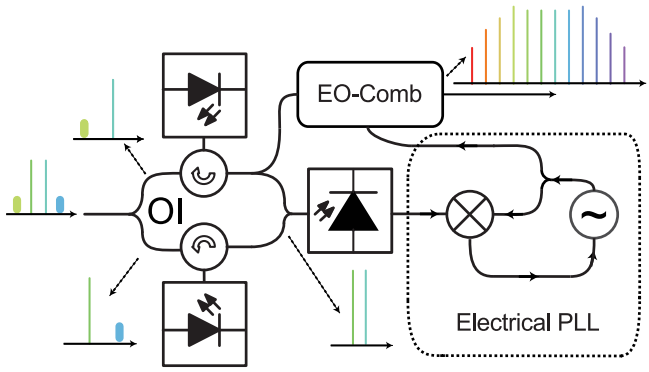

Fig. 4. Schematic of the experimental setup used to enable frequency comb regeneration. The incoming pilot tones carries the information required to fully characterize the transmitter comb. Using optical injection locking and anelectrical phase-locked loop, this information is extracted and used to phaselock a receiver electro-optic frequency comb to the transmitter frequency comb.

1 MHz) to the incoming pilot tones using an injection ratio of about -30 dB. The slave laser output in the upper arm, corresponding to the carrier feeding the transmitter comb, was divided using a 10 dB coupler with the 90% output used as optical input to the receiver EO comb.

The RF clock from the transmitter comb was extracted by combining the other output of the coupler in the upper arm with the output of the lower arm onto a photo diode with 30 GHz analog bandwidth. The resulting RF signal was then combined in a 25 GHz RF mixer with the clock signal from the receiver comb RF clock and the difference signal was used as input to an electrical phase-locked loop (PLL) used to lock the receiver clock to the transmitter clock. The PLL was of P-type and built using a voltage-controlled oscillator with 1 MHz/V gain. The PLL ensured narrow-band filtering to suppress any distortions from transmitting the pilot tones and ensured that the receiver clock tracked any drifts of the transmitter clock. No additional low-frequency clock synchronization was used between the clocks in the transmitter and receiver comb.

III. Result

Here we provide a detailed study of the performance of the electrical phase-locked loop used for regenerating the RF clock as well as the performance of the proposed superchannel transceiver scheme by means of data transmission. First, measurements of the noise spectrum for the RF clock are presented followed by back to back results from noise loading evaluation of each data carrier. Finally, we present the results from a single span transmission experiment in which the superchannel was transmitted over 80 km SSMF.

A. PLL Performance

The importance of narrow optical filtering when performing parametric frequency comb regeneration has previously been studied in [19]. To realize high fidelity all-optical comb regeneration, Brillouin amplifiers were used to filter out the pilot tones with a filter bandwidth of about 20 MHz. Despite these narrow filters, a clear scaling is observed in implementation penalty for lines further away from the superchannel center, and due to this

the regeneration was limited to a total of 24 carriers (12 on each side of the optical pilots) [19].

To study how the combination of OIL and an electrical PLL can be used to overcome this limitation by means of providing effective filtering in the recovery of the RF clock we measured the RF spectrum of the beating between the two incoming pilot tones at 3 different locations in the regeneration structure, as shown in Fig. 5. First we measured the beating after the initial optical filters (before the OI in Fig. 4) at an optical signal to noise ratio (OSNR) of 24 dB, followed by measuring after filtering using OIL as well as after using both OIL and the electrical PLL. The effect of the filtering stages, with respect to a reference measurement of the RF spectrum for the transmitter clock, are shown in Fig. 5 and we can clearly see the narrow-band filtering achieved using OIL the electrical PLL.

The direct beating of the two lines shows a noise floor in the RF spectrum of about 115 dBc/Hz. Filtering using OIL smooths this and with the injection ratio of -30 dB used in this experiment we achieved a resulting filter bandwidth on the order of 100 MHz. The filter bandwidth can be narrowed by increasing the injection ratio at the expense of reduced stability [26]. This issue can, however, be mitigated at the expense of increased complexity by using a PLL to stabilize the slave laser operation at very low input power but the resulting bandwidth is still on the order of tenths to hundreds of MHz [27]. As seen in Fig. 5, the electrical PLL achieved narrow-band filtering with a resulting bandwidth in the order of MHz, two orders of magnitude narrower the case of using only OIL to filter out the tones. The small jumps and variations around 1 MHz in Fig. 5 are caused by the electrical spectrum analyzer used which introduced discontinuities in the spectrum at 1 MHz. The PLL filtering can be slightly improved using a smaller locking range. The drawback of using a more narrow-band PLL lines in the ability to track drifts from the transmitter comb RF clock and extra distortions introduced by the OIL. As a result of this, optimal locking bandwidth will be a function of both and depends of the combined stability of both subsystems.

B. Back-to-Back Evaluation

To evaluate performance channel by channel we used the noise loading setup described in Section II-A. First we performed noise loading of the data carriers without adding any noise to the pilot tones (OSNR of the pilot tones was >30 dB) and we found that an OSNR of about 24 dB for the data carriers was needed to reach the BER target of $2.7 \cdot 10^{-2}$. After this, we noise loaded the pilot tones to a corresponding OSNR of 24 dB. At this level we then performed a noise loading sweep for each carrier to study variations among the different data carriers within the superchannel. The OSNR penalty, with respect to the theoretical value of 19.8 dB, for the cases of no noise and and OSNR of 24 dB for the pilot tones are shown in Fig. 6(a) together with difference between the two. We observe a fairly large penalty with a minimum and mean implementation penalty of 3.5 dB and 5.1 dB, respectively. The small difference observed between a pilot tone OSNR of >30 dB and 24 dB is due to the narrow filtering provided by the use of OIL and the

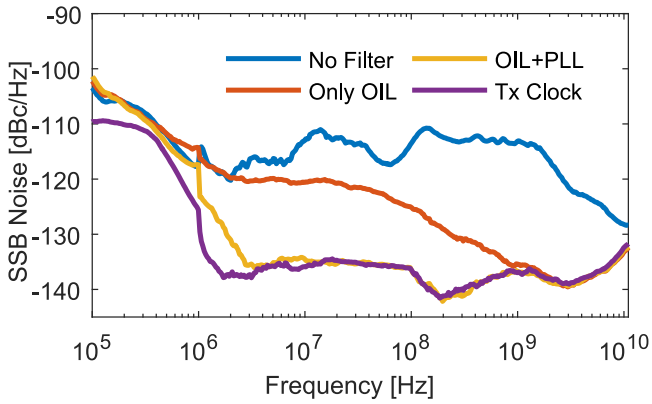

Fig. 5. Comparison between the frequency noise of the RF signal measured at different points in the regeneration setup. Beating of incoming tones before regeneration (blue), beating of tones after filtering using optical injection locking (red), beating of tones after filtering using optical injection locking and the electrical phase-locked loop (yellow) and the reference spectrum for the RF clocked used in the transmitter comb (purple).

PLL. As a result of this, the difference is due to measurement uncertainties rather than additional noise.

The large penalty observed in Fig. 6(a) is mainly the result of practical constrains in the experimental design. As mentioned in Section II-A, the pre-modulation EDFA had large gain variations over the spectral band occupied by the comb source. To overcome this and ensure equal carrier power into the modulators a flattening stage was used. This resulted in an input power into the pre-modulation EDFA of about 0 dBm with around 15 dB power variations among the lines. Taking into account an EDFA noise figure of about 5 dB, the OSNR per carrier varied from about 30 to 45 dB. In addition, the achievable OSNR for all lines was further limited by the use of only two modulators. The input power into each modulator was limited to 20 dBm and the total loss of the modulators together with the polarization emulation stages was about 25 dB each. The post-modulation EDFA had a noise figure of about 5 dB over the spectral band used and as a combined result of this, the maximum achievable OSNR was limited to about 35 dB without accounting for the prior OSNR degradation.

Neither the limitation in achievable OSNR nor the variations between individual carriers were accounted for in the noise-loading stage and thus directly transfers to varying implementation penalty among the lines and an over-estimation penalty compared to the case of single carrier. The LO OSNR also varied within the superchannel due to varying line power prior to selection and limited input power of 20 dBm the comb. The maximum line difference within the comb was around 12 dB and the absolute line power drifted around 3 dB for both combs within the time required to measure the noise loading sweeps. These variations on both the transmitter and receiver side also caused slightly varying effective OSNRs for all lines, contributing to the varying penalty observed in Fig. 6. To isolate penalties from the superchannel setup (e.g., combs, flattening stages, filters) we measured the implementation penalty for the case of directly connecting the laser to the modulator and using this same laser as local oscillator. The measured implementation

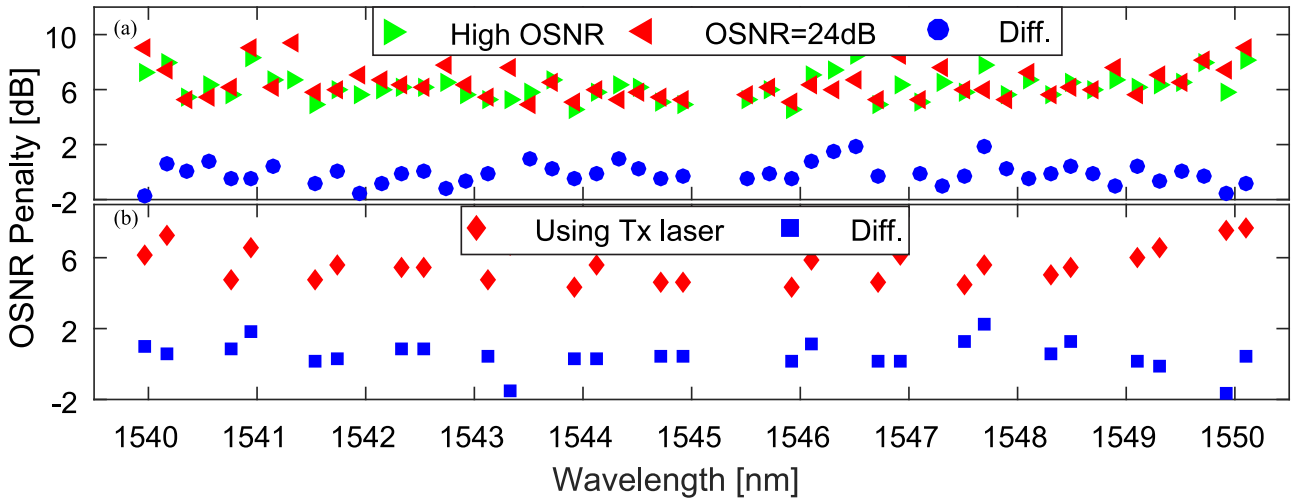

Fig. 6. OSNR penalty with respect to the theoretical required OSNR of 19.8 dB at a BER of $2.7 \cdot 10^{-2}$ in back to back configuration. (a) OSNR penalty for the receiver using frequency comb regeneration with and without noise added to the pilot tones. (b) OSNR penalty from regenerating only the frequency spacing and using the same master laser for both the transmitter and receiver combs. The variations indicate that further optimization is needed to ensure stable performance over long time for the locking of the slave laser.

penalty with regard to the theoretical value was 2 dB, which confirms that driving signal and processing at the receiver were not causing a major implementation penalty.

In order to isolate penalties from the regeneration we carried out an additional noise loading experiment to separate penalty from the transmitter itself, regenerating the central carrier feeding the comb and the frequency spacing given by the RF clock. Instead of using the regenerated central carrier to feed the receiver comb we put a tap on the laser feeding the transmitter comb and used it for both combs. Without adding any noise to the pilot tones we then studied the implementation penalty for the data carriers and compared it to the case of using the regenerated carrier to feed the receiver comb. The penalty with respect to theory as well as the difference between using the transmitter laser and the regenerated laser for 28 data carriers are shown in Fig. 6(b). Using the slave laser output to feed the receiver EO comb resulted in a mean penalty of 0.5 dB. This shows that even without noise loading, a small but noticeable part of the implementation penalty originates from the slave laser seeding the receiver comb. Reference measurements with comb-based intradyne detection revealed issues with frequency stability which caused issues with equalizer convergence as well as carrier recovery. As a result of this, no direct comparison could be made.

The variations between carriers in Fig. 6(b) were observed over a time scale of hours and polarization fluctuations before the OIL locking contributed to this drift by changing the slave laser input power. The measurements shown in Fig. 6 were automatized serial measurements without realigning the polarization in between measuring each line. It took about 20 minutes to measure each line and temperature variations therefore caused polarization fluctuations on the pilot tones. These variations could, however, be avoided by employing active polarization tracking on the input to the slave lasers and this will be needed to ensure long-term stability in an environment where the state of polarization of the pilot tones varies with time.

C. 80 km Transmission Experiment

As a final demonstration we transmitted the superchannel over 1 span of 80 km SSMF. The launch power was optimized using a launch power sweep between 7 dBm and 14 dBm, corresponding to a power per channel between -10 dBm and -3 dBm, respectively. The resulting BERs for all 50 data channels are shown in Fig. 7(a). The average BER for all 50 data channels versus launch power is plotted in Fig. 7(b) and the optimal launch power was found to be 10 dBm. Individual launch power sweeps for 4 wavelength channels (1540.8 nm, 1542.7 nm, 1544.3 nm and 1547.1 nm) are shown in Fig. 7(c).

From Fig. 7(a) and (b), we can observe similar results for high launch powers as previously reported for regeneration using a parametric receiver comb in [19]. The penalty from increasing the launch power grows rapidly when going beyond optimal and we found the optimal launch power of 10 dBm seems to be slightly lower than for similar intradyne systems. How this penalty is divided between effects on the data carriers and on the pilot tones prior to regeneration is still an open question and further studies on how distortions on the optical pilot tones are transferred to the data channels through the regeneration process is needed to clarify this.

The resulting BER and GMI after 80 km transmission at optimal launch power are shown Fig. 8(a) and (b) respectively. As seen in Fig. 8(b), all lines have a GMI well above the 10 bit/4D-symbol required for 20% FEC overhead. The minimum and average BERs were $1.3 \cdot 10^{-2}$ and $1.9 \cdot 10^{-2}$, respectively, and the corresponding values for the GMI were 10.7 bits/4D-symbol. Combining all the 50 carriers within the superchannel with 20% FEC overhead results in a total aggregated data rate of 10 Tb/s. The total GMI combined for all the data carriers was 555 bits/s resulting in a total data rate of 11.1 Tb/s assuming individual optimized FEC with bit-wise decoding for each data carrier [28]. Constellation diagrams for the X-polarization of 4 selected wavelengths (1540.4 nm, 1543.5 nm, 1547.5 nm and

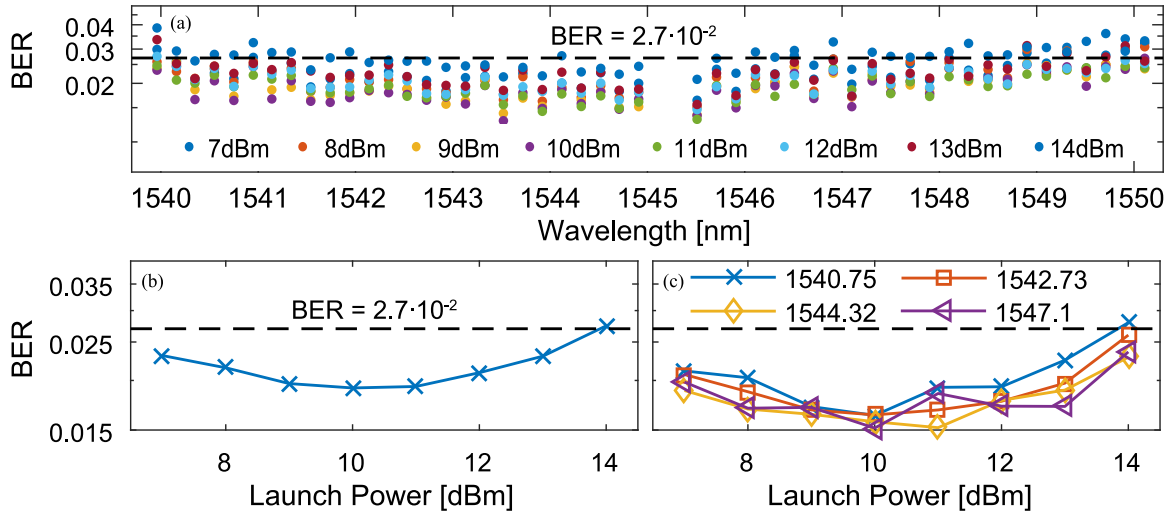

Fig. 7. Results for all 50 data carriers after 80 km transmission. (a) BER as a function of total channel launch power (steps of 1 dB from 7 dBm to 14 dBm). (b) Average BER over all channels for each launch power. (c) Example of individual launch power curves for channels at 1540.8 nm, 1542.7 nm, 1544.3 nm and 1547.1 nm.

1550.1 nm) after 80 km transmission at optimal launch power are shown in Fig. 9.

IV. Discussion

In this paper, we have proposed and evaluated a scheme for enabling self-homodyne transmission of superchannels using frequency combs. The scheme is based on using two optical pilot tones to transmit frequency and phase information of the comb used as a coherent light source in the transmitter to the receiver as proposed in [19], [21], but differs fundamentally in the regeneration scheme. Here we proposed and evaluated the use of an electrical PLL to achieve narrow-band filtering to recover the RF clock.

Systems like the one proposed in this work aims at an operating regime in which available spectrum is the main limited resource. With the powerful and energy-efficient DSP available, optical pilots will only be considered if they can reduce the total overhead compared to the case of standard approaches using independent lasers. The major part of this overhead is, naturally, the loss in throughput due to the allocation of spectral bandwidth for pilot transmission but from a broader perspective, the overhead includes both the loss in throughput and the additional resources needed to transmit, recover and utilize the optical pilot tones. In this demonstration, a total SE of 7.7 bits/s/Hz was achieved. The overheads limiting the spectral efficiency was 20%, 25% and 4% for FEC, inter-channel guard-band and pilot tone transmission, respectively. To increase the spectral efficiency even further the total OH has to be reduced. Instead of a fixed FEC OH determined by the worst performing channel, the total FEC OH could be reduced using performance dependent FECs for each channel. The OH for inter-channel guard-bands was the largest OH and hence resulting in the largest degradation in the SE. This OH could be lowered by increasing the baud-rate of the channels, similar to [29]. The trade-off is an increased cross-talk from neighboring channels due to the smaller guard-bands. As discussed in Section III-B, our transmitter already had a fairly large implementation penalty and to focus on the conceptual demonstration we therefore used a larger guard-band. To fully optimize the spectral efficiency, the inter-channel guard-band and FEC OH should be jointly optimized.

While both the FEC and guard-band OH were significantly larger than the pilot tone OH, the key aspect of this work is to reduce the OH for self-homodyne detection. This OH can be reduced using two key approaches. First, an OH reduction can be achieved by increasing the number of data channels, which share the pilot tones. This can be realized by either using a broader comb source or making use of the spatial domain if SDM fibers are used, as discussed in Section I. In the case of a broader comb source, we should also consider whether having a broader comb causes any further noise degradation due to e.g., increased phase noise for the outer lines. The other strategy to reduce the OH is to reduce the spectral loss from inserting the pilot tones. Once such way would be to use 2 data carriers with lower symbol rate around the two central lines, allowing for an up- or down-shifted pilot tone within the channel bandwidth, similar to [30], [31]. This would allow for a reduction in OH at the expense of extra complexity due to the requirement of frequency shifting stages. To extract the RF clock a minimum of two pilot tones are required. Although the two tones were placed in the middle of the superchannel in this work, they can in theory be placed elsewhere. Depending on the comb technology used, phase noise scaling could be present and depending on the strength of this effect, a more centralized position might be beneficial. On the other hand, centralized placement implies that the tones suffer the most from nonlinear effect, which depending on link length and design, could affect the performance.

Dispersive walk-offs between both the pilot tones and between the tones and the data channels will eventually limit the performance of the proposed scheme. Gradually, these walk-offs will limit the achievable phase coherence between the transmitter and receiver comb, leading to increased presence of phase noise in the data after detection. At what point this will start to

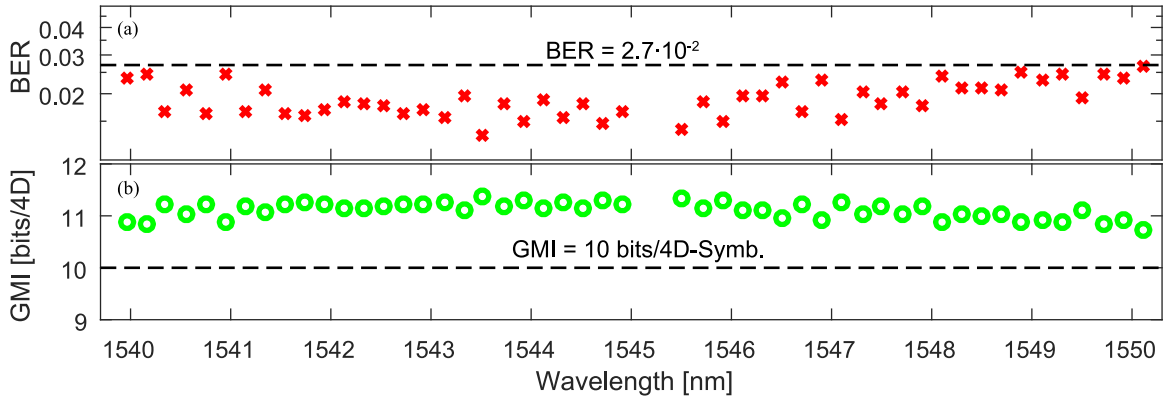

Fig. 8. Results for all 50 data carriers after 80 km transmission at optimal launch power of 10 dBm. (a) and (b) shows the BER and GMI, respectively, for all 50 data channels. All channels are well below the BER target for 20% coding overhead and the large margin in terms of GMI further verifies this. Allocating a 20% overhead for FEC results in a total superchannel transmission rate of 10 Tb/s.

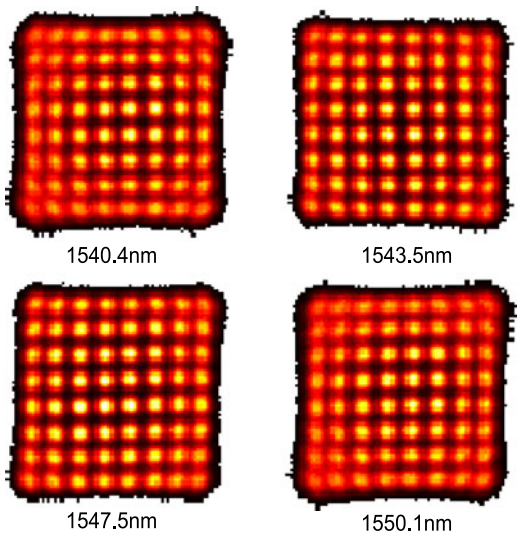

Fig. 9. Received constellation diagrams (X-polarization) for the wavelength channels 1540.4 nm, 1543.5 nm, 1547.5 nm and 1550.1 nm. The constellations were weasured at optimal launch power of 10 dBm, corresponding to −7 dBm per channel.

limit the performance depends naturally on the dispersion parameters of the fiber used as well as link length. The linewidth of the transmitter comb seed laser is also crucial to this penalty and increased tolerance can be gained by employing a high quality, narrow linewidth laser source. Linewidth degradation of the re-generated comb due to walk-off between the pilot tones was previously studied in [21] for the case of parametric regeneration. While the fundamental aspects are the equivalent in the case of regeneration using OIL and the proposed phase-locked loop, it remains an open question how tolerant this scheme is to dispersive walk-offs. Optical dispersion compensation could be used to suppress penalties from dispersion walk-off at the expense of increased sensitivity to nonlinear effects.

Worth pointing out here is that the proposed scheme eliminates the DSP-based carrier recovery and simplifies the use of higher-order modulation formats. Since these formats are fundamentally more sensitive to noise, being either amplifier noise, phase noise or nonlinear noise-like impairments, the scheme is most suitable for shorter systems. For long-haul systems without optical dispersion compensation, the power consumption of the electronic dispersion compensation is about one order of magnitude larger than the one for carrier recovery [3] and the extra complexity of comb regeneration makes the scheme fundamentally less attractive.

The optimal launch power found here for the case of single span transmission seems to be slightly lower than what one would expect for an equivalent intradyne DWDM system. This follows previously observed results for the case of parametric comb regeneration [19]. Whether or not this is due to the use of correlated data channels [32], nonlinear distortions on the pilot tones that gives raise to extra noise contributions, inability to compensate nonlinear phase noise due to the lack of DSP-based phase tracking [33], [34] or something else remains to be investigated. Aspects such as power ratio between pilot tones and data channels, pilot tone placement, number of channel within the superchannel and link design are all likely to influence the sensitivity to fiber nonlinearities. Which one of these, if any, being the dominant one is also likely to depend strongly on link-specific aspect such as total length, span length and which amplification scheme being used.

V. Conclusion

In this work we have provided a proof-of-principle demonstration of frequency comb regeneration using an electrical phase-locked loop for self-homodyne superchannel transmission. The superchannel was formed from 52 lines originating from a common frequency comb. Two central lines were left unmodulated and used as optical pilot tones, and the remaining lines were modulated using 20 Gbaud PM-64QAM. The pilot tones were used in the receiver together with optical injection locking and the phase-locked loop to lock a receiver comb to the transmitter comb. Self-homodyne transmission with a spectral overhead of 4% was demonstrated over a single span of 80 km standard single-mode fiber. The total superchannel throughput was 10 Tbit/s with a corresponding spectral efficiency of 7.7 bits/s/Hz. This demonstrates that frequency combs in combination with optical pilot tones can be used to exploit the benefits of self-homodyne detection to enable detection of

high-order QAM modulation formats while keeping the pilot overhead low.

REFERENCES

[1] C. Laperle and M. Osullivan, "Advances in high-speed DACs, ADCs, and DSP for optical coherent transceivers," *J. Lightw. Technol.*, vol. 32, no. 4, pp. 629–643, Feb. 2014.

[2] S. Wolf *et al.*, "Silicon-oganic hybrid (SOH) IQ modulator for 100 GBd 16QAM operation," in *Proc. Opt. Fiber Commun. Conf. Exhib.*, 2017, Paper Th5C.1.

[3] B. S. G. Pillai *et al.*, "End-to-end energy modeling and analysis of long-haul coherent transmission systems," *J. Lightw. Technol.*, vol. 32, no. 18, pp. 3093–3111, Sep. 2014.

[4] T. Rahman *et al.*, "Long-haul transmission of PM-16QAM , PM-32QAM and PM-64QAM based terabit superchannels over a field deployed legacy fiber," *J. Lightw. Technol.*, vol. 34, no. 13, pp. 3071–3079, Jul. 2016.

[5] J.-X. Cai *et al.*, "70.46 Tb/s over 7,600 km and 71.65 Tb/s over 6,970 km transmission in c+l band using coded modulation with hybrid constellation shaping and nonlinearity compensation," *J. Lightw. Technol.*, vol. 36, no. 1, pp. 114–121, Jan. 2018.

[6] P. J. Winzer and D. T. Neilson, "From scaling disparities to integrated parallelism: A decathlon for a decade," *J. Lightw. Technol.*, vol. 35, no. 5, pp. 1099–1115, Mar. 2017.

[7] L. Lundberg, M. Mazur, A. Lorences-Riesgo, M. Karlsson, and P. A. Andrekson, "Joint carrier recovery for DSP complexity reduction in frequency comb-based superchannel transceivers," in *Proc. Eur. Conf. Opt. Commun.*, 2017, Paper Th.1.D.3.

[8] T. Miyazaki and F. Kubota, "PSK self-homodyne detection using a pilot carrier for multibit/symbol transmission with inverse-RZ signal," *IEEE Photon. Technol. Lett.*, vol. 17, no. 6, pp. 1334–1336, Jun. 2005.

[9] M. Sjödin, E. Agrell, P. Johannisson, G.-W. Lu, P. A. Andrekson, and M. Karlsson, "Filter optimization for self-homodyne coherent WDM systems using interleaved polarization division multiplexing," *J. Lightw. Technol.*, vol. 29, no. 9, pp. 1219–1226, May 2011.

[10] B. J. Puttnam *et al.*, "Investigating self-homodyne coherent detection in a 19 channel space-division-multiplexed transmission link," *Opt. Express*, vol. 21, no. 2, pp. 1561–1566, 2013.

[11] J. M. D. Mendinueta *et al.*, "Investigation of receiver DSP carrier phase estimation rate for self-homodyne space-division multiplexing communication systems," in *Proc. Optical Fiber Commun. Conf.*, 2013, Paper Th2A.48.

[12] A. F. Alfredsson, R. Krishnan, and E. Agrell, "Joint-polarization phase-noise estimation and symbol detection for optical coherent receivers," *J. Lightw. Technol.*, vol. 34, no. 18, pp. 4394–4405, Sep. 2016.

[13] R. S. Luís *et al.*, "Time and modulation frequency dependence of crosstalk in homogeneous multi-core fibers," *J. Lightw. Technol.*, vol. 34, no. 2, pp. 441–447, Jan. 2016.

[14] R. S. Luís, B. J. Puttnam, J. M. D. Mendinueta, Y. Awaji, and N. Wada, "Impact of spatial channel skew on the performance of spatial-division multiplexed self-homodyne transmission systems," in *Proc. Int. Conf. Photon. Switching*, 2015, pp. 37–39.

[15] S. Beppu, K. Kasai, M. Yoshida, and M. Nakazawa, "2048 QAM (66 Gbit/s) single-carrier coherent optical transmission over 150 km with a potential SE of 15.3 bit/s/Hz," *Opt. Express*, vol. 23, no. 4, pp. 4960–4969, 2015.

[16] K. Kasai, M. Yoshida, T. Hirooka, and M. Nakazawa, "Injection-locked homodyne detection system for higher-order QAM digital coherent transmission," in *Proc. Eur. Conf. Opt. Commun.*, 2016, Paper M.1.C.3.

[17] T. Pfau, S. Hoffmann, and R. Noé, "Hardware-efficient coherent digital receiver concept with feedforward carrier recovery for M-QAM constellations," *J. Lightw. Technol.*, vol. 27, no. 8, pp. 989–999, Apr. 2009.

[18] B. Puttnam *et al.*, "2.15 Pb/s transmission using a 22 core homogeneous single-mode multi-core fiber and wideband optical comb," in *Proc. Eur. Conf. Opt. Commun.*, 2015, Paper PDP3.1.

[19] A. Lorences-Riesgo, M. Mazur, T. A. Eriksson, P. A. Andrekson, and M. Karlsson, "Self-homodyne 24x32-QAM superchannel receiver enabled by all-optical comb regeneration using Brillouin amplification," *Opt. Express*, vol. 24, no. 26, pp. 29 714–29 723, 2016.

[20] A. C. Bordonalli, M. J. Fice, and A. J. Seeds, "Optical injection locking to optical frequency combs for superchannel coherent detection," *Opt. Express*, vol. 23, no. 2, pp. 1547–1557, 2015.

[21] A. Lorences-Riesgo, T. A. Eriksson, A. Fülöp, P. A. Andrekson, and M. Karlsson, "Frequency-comb regeneration for self-homodyne superchannels," *J. Lightw. Technol.*, vol. 34, no. 8, pp. 1800–1806, Apr. 2016.

[22] M. Mazur, A. Lorences-Riesgo, M. Karlsson, and P. A. Andrekson, "10 Tb/s self-homodyne 64-QAM superchannel transmission with 4% spectral overhead," in *Proc. Opt. Fiber Commun. Conf.*, 2017, Paper Th3F.4.

[23] A. J. Metcalf, V. Torres-Company, D. E. Leaird, and A. M. Weiner, "High-power broadly tunable electrooptic frequency comb generator," *J. Select. Topics Quantum Electron.*, vol. 19, no. 6, pp. 231–236, 2013.

[24] D. Chang *et al.*, "LDPC convolutional codes using layered decoding algorithm for high speed coherent optical transmission," in *Proc. Opt. Fiber Commun. Conf.*, 2012, Paper OW1H.4.

[25] A. Alvarado, E. Agrell, D. Lavery, R. Maher, and P. Bayvel, "Replacing the soft-decision FEC limit paradigm in the design of optical communication systems," *J. Lightw. Technol.*, vol. 34, no. 2, pp. 707–721, Jan. 2016.

[26] K. Kasai, Y. Wang, S. Beppu, M. Yoshida, and M. Nakazawa, "80 Gbit/s, 256 QAM coherent transmission over 150 km with an injection-locked homodyne receiver," *Opt. Express*, vol. 23, no. 22, pp. 29174–29183, 2015.

[27] D. S. Wu, R. Slavík, G. Marra, and D. J. Richardson, "Direct selection and amplification of individual narrowly spaced optical comb modes via injection locking: Design and characterization," *J. Lightw. Technol.*, vol. 31, no. 14, pp. 2287–2295, Jul. 2013.

[28] A. Ghazisaeidi *et al.*, "Transoceanic transmission systems using adaptive multirate FECs," *J. Lightw. Technol.*, vol. 33, no. 7, pp. 1479–1487, Apr. 2015.

[29] S. Chandrasekhar *et al.*, "High-spectral-efficiency transmission of PDM 256-QAM with parallel probabilistic shaping at record rate-reach trade-offs," in *Proc. Eur. Conf. Opt. Commun.*, 2016, Paper Th.3.C.1.

[30] Y. Wang, K. Kasai, M. Yoshida, and M. Nakazawa, "320 Gbit/s, 20 Gsymbol/s 256 QAM coherent transmission over 160 km by using injection-locked local oscillator," *Opt. Express*, vol. 24, no. 19, pp. 22088–22096, 2016.

[31] T. Kan, K. Kasai, M. Yoshida, and M. Nakazawa, "42.3 Tbit/s, 18 Gbaud 64 QAM WDM coherent transmission over 160 km in the C-band using an injection-locked homodyne receiver with a spectral efficiency of 9 bit/s/Hz," *Opt. Express*, vol. 25, no. 19, pp. 22726–22737, 2017.

[32] R. Dar *et al.*, "Impact of WDM channel correlations on nonlinear transmission," in *Proc. Eur. Conf. Opt. Commun.*, 2016, pp. 1–3.

[33] F. P. Guiomar, A. Carena, G. Bosco, L. Bertignono, A. Nespola, and P. Poggiolini, "Nonlinear mitigation on subcarrier-multiplexed PM-16QAM optical systems," *Opt. Express*, vol. 25, no. 4, pp. 4298–4311, 2017.

[34] T. Fehenberger, N. Hanik, T. A. Eriksson, P. Johannisson, and M. Karlsson, "On the impact of carrier phase estimation on phase correlations in coherent fiber transmission," in *Proc. Tyrrhenian Int. Workshop Digital Commun.*, 2015, pp. 35–38.

Authors' biography not available at the time of publication.